Bol. Inst. Esp. Oceanogr. 15 (1-4). 1999: 61-72 **BOLETÍN** INSTITUTO ESPAÑOL DE OCEANOGRAFÍA
ISSN: 0074-0195

The slope current along the western European margin: A numerical investigation

H. S. Coelho[1], *R. R. Neves*[2], *P. C. Leitão*[2], *H. Martins*[2] *and A. P. Santos*[2]

[1] Algarve University, Campus de Gambelas, 8000 Faro, Portugal
[2] Mechanical Engineering Department, Instituto Superior Técnico, Av. Rovisco Pais, 1096 Lisboa, Portugal

Received October 1997. Accepted March 1998.

ABSTRACT

A three-dimensional hydrodynamic model is used to investigate the poleward flow along the western European slopes. The area of the model domain goes from northwest Africa to Ireland. During a first stage, the currents are driven by climatological density fields. In a second stage the model is also forced by climatological winds, although special attention is paid to spring, when the winds are favourable to the development of an equatorward jet along the Iberian coast.

Results show that the climatological density field is able to produce the poleward current along the European continental slope. Winds can modify the flow pattern, mainly in the southern areas off Iberia, specially during the upwelling season.

The poleward current obtained is continuous between the Portuguese and French coasts, following the contour depths, with a core of maximum velocity located from 300-1 500 m, depending both on space and time. This core corresponds to the shelfward divergence of isopycnals. Maximum speeds range from 10-20 cm/s. A poleward intensification of the current is also obtained.

Key words: Ocean circulation modelling, continental margin, poleward flows.

RESUMEN

Las corrientes de talud a lo largo del margen occidental europeo: una investigación numérica

Un modelo tridimensional hidrodinámico se ha usado para investigar el flujo en dirección hacia el polo a lo largo del talud occidental europeo. El área de dominio del modelo va desde el noroeste de África hasta Irlanda. En un primer estadio, las corrientes son dirigidas por los campos climatológicos de densidad. En un segundo estadio el modelo se fuerza con vientos climatológicos, donde se presta una especial atención a la primavera, cuando los vientos son favorables al desarrollo de un jet *en dirección al ecuador a lo largo de la costa ibérica.*

Los resultados muestran cómo el campo de densidad climatológica es capaz de producir una corriente en dirección al polo a lo largo del talud del continente europeo. Los vientos pueden modificar este esquema de flujo, principalmente en las áreas al sur de la península Ibérica, sobre todo durante la estación de upwelling.

La corriente hacia el polo obtenida es continua entre las costas portuguesa y francesa, siguiendo las líneas de profundidad, con una velocidad máxima en el núcleo situada entre 300 m y 1 500 m, dependiendo tanto del espacio como del tiempo. Este núcleo corresponde a la divergencia de las isopicnas hacia la plataforma continental. Las velocidades máximas varían entre 10 y 20 cm/s. También se obtiene una intensificación hacia el polo de la corriente.

Palabras clave: *Modelización de la circulación oceánica, margen continental, flujos hacia el polo.*

INTRODUCTION

The presence of sloping bathymetry along the continental margin, combined with the general circulation, generates a complex flow pattern along the slope regions. This flow is characterised by major vertical and horizontal gradients of velocity and density, producing eddies, fronts, instabilities and other related phenomena. The understanding of these processes, as well as their quantification and integration, is not easy. Numerical models can be an appropriate tool both for process studies and for interdisciplinary integration of results.

The present paper reports on a project undertaken within the framework of the 'Ocean Margin Exchange' (OMEX) programme, with the main objective of studying the generation, development and persistence of the poleward current along the western European margin. Special attention is paid here to the flow off the western Iberian Peninsula.

Observations of poleward flows along eastern ocean boundaries

Frouin *et al.* (1990) presented evidence of a warm and salty surface current along the Iberian Peninsula's upper continental slope and outer continental shelf during the winter of 1983-1984. The characteristics of the water advected are typical of the sub-tropical waters formed near the Azores. Haynes and Barton (1990), using satellite imagery and Lagrangian drifters, observed a northward flow off Iberia, between September 1986 and March 1987, whose characteristics are similar to those described by Frouin *et al.* (1990). In their work using current-meter data, Haynes and Barton (1990) identified the presence of Mediterranean Intermediate Water (MIW) at depths greater than 600 m. Previous work by Ambar (1984, 1985) indicates that the poleward flow may extend from the bottom of MIW (1 600 m) to the bottom of the surface layer. Ambar *et al.* (1986) also observed a similar flow during the winter of 1983. Analysis of satellite images indicates that this situation occured between November and March nearly every year between 1982 and 1990.

It seems that the surface poleward flow along the Iberian upper continental slope and outer continental shelf, during the winter, is a regular pattern. It is also noteworthy that all observational evidence indicates that during the upwelling season, deep waters still flow poleward. Even more remarkable is the occurrence of poleward currents in other ocean eastern boundaries at subtropical and mid-latitudes. Lynn and Simpson (1987) investigated the seasonal cycle of the flow within the California Current System (CCS), and concluded that it is characterised by the appearance of what they called the Inshore Countercurrent (IC) and by the intensification of the California Undercurrent (CU). Evidence also suggests that the appearance of the IC is associated with the shoaling of the CU. This means that the flow is poleward throughout the year, being an undercurrent during the upwelling season and a surface countercurrent (also known as the Davidson Current) between October and March (the non-upwelling season). A similar current was found off western Canada, called the Haida Current (Thomson and Emery, 1986).

The west coast of Australia is also a subtropical eastern boundary, even though it experiences year-round equatorward winds. Its coastal circulation is characterised by a narrow surface poleward flow, called the Leeuwin Current (Thompson, 1984). This flow intensifies as it flows poleward, despite the opposing wind, attaining its maximum strength in the austral winter, when the alongshore winds are weakest.

There are also numerous observations of poleward flows along the continental slope of the eastern boundary throughout the North Atlantic subtropical gyre. Pingree and LeCann (1989, 1990) summarised current-meter data collected over 20 years and found a consistent poleward current along the Armorican and Celtic slopes.

In summary, many authors have provided evidence of a poleward flow along European slopes (Ambar *et al.*, 1986; Huthnance, 1986; Frouin *et al.*, 1990; Haynes and Barton, 1990; Pingree and LeCann, 1989). Very similar poleward flows have been described in other eastern boundary regions, such as the aforesaid CCS and the west coast of Australia. These flows, mainly concentrated along the upper continental slope and outer continental shelf, sometimes appear as an undercurrent and sometimes as a surface current, depending both on the studied region and the time of the year. These currents exist on the thermal layer of the ocean (upper 1 000 m). Barton (1989) suggested the continuity of the poleward flow along the en-

tire eastern boundary, and attributed to the Iberian poleward flow a determinant role for the advection of Mediterranean water, ultimately, into the Norwegian Sea.

Characteristics of the poleward current off Iberia

The Iberian poleward current runs for 1 500 km along the upper continental slope –shelf-break zone– of western Portugal, northwest Spain, northern Spain and southwest France, and is 25-40 km wide. Frouin *et al.* (1990) described a flow 200 m deep, but other reports suggest that the current extends from the bottom of MIW (1 600 m) to the bottom of the surface layer during the upwelling season, and to the surface during the non-upwelling season. The current is characterised by velocities ranging from 0.2-0.3 m/s. The associated transports are, according to Frouin *et al.* (1990), 300×10^3 m^3/s at about 38° N and 500-700 $\times 10^3$ m^3/s at about 41° N. This means that the current intensifies poleward, which is also a characteristic of the poleward currents at the eastern boundaries.

Generation mechanisms

Several driving mechanisms have been proposed over the past 20 years to explain slope currents around the World Ocean. Clarke (1989) listed the main mechanisms that can force mean flows along the eastern ocean boundaries. He included tidal rectification, melting ice and rivers emptying into the sea, forcing by offshore mean density gradients, non-linear interaction between forced barotropic shelf waves over the continental margin, and mean wind-stress and wind-stress curl. Clarke concentrated his discussion on the dynamics of poleward flowing undercurrents on eastern ocean boundaries, and excluded mechanism like melting ice, rivers and tidal rectification. He argued that melting ice and rivers can only produce surface currents, and tidal rectification is only important when both the tidal currents and bottom topography slope are large. Based on *in situ* observations, satellite imagery and numerical model applications some of these mechanisms have been studied and some of them excluded. Frouin *et al.* (1990) considered three basic mechanisms: thermohaline forcing, wind forcing and dam break. They excluded dam break due to strong discrepancies between the available models and their observations. The most considered mechanisms driving alongshore currents are wind-stress and wind-stress curl and thermohaline forcing.

Wind-stress and wind-stress curl

Ambar *et al.* (1986) associated the surface poleward current off Iberia during the winter of 1983 with the northward wind-stress prevailing at that time of year. Indeed, onshore Ekman convergence induced by south-southwesterly wind provides a possible explanation for poleward surface flow. The shelfward transport induced by this kind of wind causes a sea- level rising near the coast. The geostrophic adjustment to this sea-level distribution will then generate a poleward current. In this case the alongshore acceleration is given by $\frac{\partial V}{\partial t} = \frac{\tau^y}{\rho H}$ being H the depth of the frictional layer, V the alongshore velocity, t the windstress and r the seawater density. Frouin *et al.* (1990) used t = 0.03 Nm^{-2}, r = 1027 kg m^{-3} and H = 200 m to find that the alongshore acceleration is 0.013 m s^{-1} day^{-1}, which gives V = 0.4 m s^{-1} after 30 days. However they argued that other effects, in particular friction, retard the flow. Assuming a steady state reached when the bottom stress balances the windstress $\left(C_b V^2 = \frac{\tau^y}{\rho}\right)$, they obtained V ≅ 0.17 m s^{-1}, which was in agreement with their observations. This current should decay seaward from the shelf break. The spatial scale associated with the decay of the current is the internal radius of deformation (about 15 km off the Iberian Peninsula). This is generally what is observed both with satellite images and *in situ* observations. When Frouin *et al.* (1990) evaluated the Ekman volume transported by the current, they found that this mechanism provides only one-fifth of the observed transports, and concluded that this could not be the main driving mechanism for the poleward current.

McCreary, Kundu and Chao (1987), using ocean models, proposed that the most likely cause of the Davidson Current off California was a positive

wind-stress curl forcing poleward Sverdrup transport. The Sverdrup relation, $\beta M_y = curl_z \tau$ (where $\beta = \frac{\partial f}{\partial y}$ and My denotes the northward volume transport), shows that the wind-stress curl alone can generate transport in the alongshore direction. Bakun and Nelson (1991) showed that the wind stress curl off the Iberian Peninsula is positive. This means that the Sverdrup mechanism is a possible cause of the poleward current along the Portuguese and northern Spanish continental slopes.

Thermohaline forcing

Several authors (e.g. Lynn and Simpson, 1987; Frouin *et al.*, 1990; Haynes and Barton, 1990) suggested that poleward currents along eastern boundaries may be associated with the large-scale eastward flow, associated with meridional pressure gradient, that occurs in the upper 200-300 m. Model results obtained by McCreary, Shetye and Kundu (1986) and Weaver and Middleton (1990) for the Leeuwin Current confirm this thesis. The poleward cooling of the sea surface leads to a meridional increase of surface density, causing the dynamic height to drop towards the pole. The result is a weak surface eastward flow from the interior to the ocean boundary, forcing coastal downwelling and a surface poleward current. This mechanism explains both the existence of the current and its increase towards the pole. We also know that, off Iberia and off California, these surface currents tend to disappear during late spring and summer. On the other hand, the Leeuwin Current weakens during the austral summer. Calculations of volume transports associated with the large-scale meridional pressure gradient in the North Atlantic suggest that it is present throughout the year and does weaken during summer (Klein and Siedler, 1989). This should lead to a northward current, even during the summer, but southward local winds tend to reverse the surface flow and produce the equatorward jet typical of upwelling situations. The Leeuwin Current is a particular case: al though equatorward winds prevail during most of the year, they are weakest in the winter.

Huthnance (1984) showed that a combination of slope bathymetry with a south-north density gradient provides a local mechanism that can drive a poleward current. It is possible to show (cf. Pingree and LeCann, 1990) that $\rho \frac{\partial \eta}{\partial y} = -h \frac{\partial \rho}{\partial y}$ (being η the sea-surface elevation and h the water depth). Therefore, sea level declines faster in deep water than in shallow water, implying a cross-slope gradient in the sea level. The existence of this gradient leads to a poleward flow along the slope bathymetry. The cross-slope sea-level gradient is proportional to distance along the slope, and has an associated increasing along-slope transport. Huthnance also showed that if the cross-shelf density diffusion is large, the along-slope current is given by:

$$v = \frac{g}{2} \frac{H}{k} \frac{H \frac{\partial \rho}{\partial y}}{\rho} \frac{h}{H} \left(1 - \frac{h}{H}\right) \qquad [1]$$

where H is the oceanic thermal layer depth and k the bottom friction coefficient. Equation [1] gives the greatest currents over the slope in intermediate water depths between 0 and the thermal layer depth. In reality, the poleward advected water has dynamic effects, introducing a baroclinic component that reinforces the flow at upper levels offshore and lower levels inshore. This results from a small cross-shelf diffusion.

MATERIALS AND METHODS

The model

The model applied in the present paper is the three-dimensional ocean circulation model (MOHID3D) developed by Instituto Superior Tecnico (IST). Detailed description of the model can be found in Santos (1995). The model has been successfully applied in varied contexts (Coelho *et al.*, 1994a; Coelho *et al.*, 1994b; Cancino and Neves, 1994). MOHID3D solves the primitive equations, using a semi-implicit finite-difference method. The horizontal resolution of the model can be constant or variable, and is limited by computational facilities and by stability criteria. In the vertical, the model uses a double sigma co-ordinate for a good simulation of topographic effects. The model applies the Boussinesq, hydrostatic and beta-plane approximations.

Equations

The model solves the equations for momentum, the equation of continuity, two transport equations

for heat and salt and an equation of state (Leendertsee and Liu, 1978), relating density to salinity and temperature:

$$\frac{\partial u}{\partial t} + u\frac{\partial u}{\partial x} + v\frac{\partial u}{\partial y} + w\frac{\partial u}{\partial z} - fv = -\frac{1}{\rho r}\frac{\partial p}{\partial x} + \\ + \frac{\partial}{\partial x}\left(A_H\frac{\partial u}{\partial x}\right) + \frac{\partial}{\partial y}\left(A_H\frac{\partial u}{\partial y}\right) + \frac{\partial}{\partial z}\left(A_V\frac{\partial u}{\partial z}\right) \quad [2]$$

$$\frac{\partial v}{\partial t} + u\frac{\partial v}{\partial x} + v\frac{\partial v}{\partial y} + w\frac{\partial v}{\partial z} + fu = -\frac{1}{\rho r}\frac{\partial p}{\partial y} + \\ + \frac{\partial}{\partial x}\left(A_H\frac{\partial v}{\partial x}\right) + \frac{\partial}{\partial y}\left(A_H\frac{\partial v}{\partial y}\right) + \frac{\partial}{\partial z}\left(A_V\frac{\partial v}{\partial z}\right) \quad [3]$$

$$\frac{\partial p}{\partial z} + \rho g = 0 \quad [4]$$

$$\frac{\partial u}{\partial x} + \frac{\partial v}{\partial y} + \frac{\partial w}{\partial z} = 0 \quad [5]$$

$$\frac{\partial (S)}{\partial t} + \frac{\partial (uS)}{\partial x} + \frac{\partial (vS)}{\partial y} + \frac{\partial (wS)}{\partial z} = \\ = \frac{\partial}{\partial x}\left(K_H\frac{\partial S}{\partial x}\right) + \frac{\partial}{\partial y}\left(K_H\frac{\partial S}{\partial y}\right) + \\ + \frac{\partial}{\partial z}\left(K_V\frac{\partial S}{\partial z}\right) + F_S \quad [6]$$

$$\frac{\partial (T)}{\partial t} + \frac{\partial (uT)}{\partial x} + \frac{\partial (vT)}{\partial y} + \frac{\partial (wT)}{\partial z} = \\ = \frac{\partial}{\partial x}\left(K_H\frac{\partial T}{\partial x}\right) + \frac{\partial}{\partial y}\left(K_H\frac{\partial T}{\partial y}\right) + \\ + \frac{\partial}{\partial z}\left(K_V\frac{\partial T}{\partial z}\right) + F_T \quad [7]$$

$$\rho = (5\,890 + 38T - 0.375T^2 + 3S)/ \\ (1\,779.5 + 11.25T - 0.0745T^2 + \\ - (3.8 + 0.01T)S + 0.698\,(5\,890 + \\ + 38T - 0.375T^2 + 3S)) \quad [8]$$

A transformation to sigma co-ordinates allows accurate resolution of complex bathymetry, transforming the real domain into a domain with constant depth. Resolving the equations in this transformed domain, the model considers the same number of layers, whatever the local depth may be. In regions where the depth varies rapidly, the thickness of each layer varies in the same way; this can be a source of numerical diffusion, large enough to make the simulation of baroclinic flows impossible without considering a very high number of layers. This is of crucial importance in places with steep slopes where the flow is driven by the density, as may be the case near the shelf break where a thermocline is usually observed, because the mesh is no longer oriented with the flow. These disadvantages of the single sigma can be improved with a double-sigma co-ordinate transformation. Beckers (1991) successfully used a model with two vertical domains to simulate the flow in the western Mediterranean, and in our work the interface of the two sigma domains is located at the level of the shelf-break.

Discretisation

To avoid iterative procedures, a time-splitting technique is used, which enabled us to solve our numerical problem by handling only tridiagonal matrixes. The time discretisation follows the S21 scheme (Abbott, Damsgaard and Rodenhuis, 1973). The explicit part of each equation includes the less stability-restrictive terms (horizontal advection and diffusion, Coriolis and baroclinic pressure). The calculation in each time step can be schematised as:

$$\eta_{ij}^{t+1/2} \rightarrow u_{ijk}^{t+1} \rightarrow w_{ijk}^{t+1/2} \rightarrow \rho_{ijk}^{t+1/2} \rightarrow \eta_{ij}^{t+1} \rightarrow \\ \rightarrow v_{ijk}^{t+3/2} \rightarrow w_{ijk}^{t+1} \rightarrow \rho_{ijk}^{t+1}$$

The need for a vertical implicit discretisation is obvious considering the Courant-Friedrichs-Lewy (CFL) criterion for advection and the stability criteria for diffusion. The implicit calculation of vertical transport is especially important in shallow areas. The same happens with bottom friction, which, if calculated explicitly, can lead to undershooting the velocity, producing unrealistic results, and even blowing up the model (Neves, 1985). For spatial discretisation, the Arakawa C grid was used. All spatial derivatives are centred, with the exception of advective terms. The ideal advection scheme would combine transportivity with low numerical diffusion. The upwind scheme satisfies the first requirement, but it can have large numerical diffusion. Central differences are less diffusive, but do not respect the transportivity property of advection and can originate negative concentrations. In the upwind calculation, the assumption is that the value on the cell surface is the value inside the cell from whence the flow is leaving. In central differences, it is assumed that the concentration is the average value between

both sides of the cell surface. In the QUICK algorithm of Leonard (1977), a quadratic interpolation is used. When the calculation is explicit, any of these methods are easily included in the model. A hybrid algorithm upwind/central difference can also be considered, using a weight factor computed with the Peclet number. In order to resolve processes with different spatial scales (domain with coastal and deep ocean regions), a uniform grid is inadequate because it would require an extraordinarily high number of points to cover the area of large-scale phenomena with the same grid size of the small-scale region. This model has the flexibility to refine the rectangular grid in regions of particular interest or in regions of large gradients.

Diffusion

Because the characteristic length scales of horizontal variations of velocity are considerably larger than vertical ones, horizontal turbulent diffusion is generally smaller than vertical. The horizontal eddy viscosity coefficient to use in the model depends on the mesh size and the turbulent energy dissipation rate ε, which in turn depends on the horizontal length scale of the model. According to Kolmogorov's theory we have:

$$A_H \approx \varepsilon^{1/3}\,\Delta^{4/3} \qquad [9]$$

For the horizontal eddy diffusivity K_H, for salt and temperature, we consider $K_H = \alpha A_H$, with $\alpha \approx 1$. As indicated above, vertical turbulent diffusion is solved implicitly, using space- and time-dependent eddy viscosity coefficients. This coefficient is generally written in the form:

$$A_V = (A_V)_{min} + (A_V)_0 \times (A_V)_S \text{ with}$$
$$(A_V)_S = (1 + \theta R_i)^{-p} \qquad [10]$$

In these equations, $(A_V)_{min}$ is a minimum limit of the eddy viscosity coefficient, $(A_V)_0$ is the vertical eddy viscosity in neutral stratification conditions, θ and p are constants, and R_i is the Richardson number. The choice of constants θ and p is part of the model calibration. According to Rodi (1980), $\theta = 10$ and $p = 0.5$ fit most of the experimental data. The value of $(A_V)_0$ must be calculated by a turbulence model. The turbulence closure used in this model is a zero-equation closure based on empirical formulae (Backhaus, 1985) or the Prandtl mixing-length formulation. Using the Prandtl mixing-length hypothesis, eddy viscosity in neutral conditions is expressed as $(A_V)_0 = l_m^2 \left|\frac{\partial U}{\partial z}\right|$. This equation relates the eddy viscosity to the local mean velocity gradient, and involves a single unknown parameter, the mixing length $l_m = H\xi\left(\frac{x_3}{H}\right)$, where $x_3 = z + h$ is the height above the bottom. For the function $\xi\left(\frac{x_3}{H}\right)$, several expressions have been proposed, such as

$$\xi = \chi \frac{x_3}{H}\left(1 - \delta \frac{x_3}{H}\right),\ 0.5 \le \delta \le 1 \text{ (Nihoul, 1982)}$$

$\chi \approx 0.4$ is the Von Karman constant. The mixing-length hypothesis is also used in heat and mass transfer. For vertical diffusivity, $K_V = A_V\,\beta(R_i)$. To account for buoyancy, several empirical formulas have been proposed, such as $\beta = \gamma \exp(-\gamma' R_i)$ with $\gamma \approx 1.4$, $\gamma' = 1.2$ (Leendertsee and Liu, 1978).

Boundary conditions

At open boundaries, a boundary condition must be imposed for the scalars (salt and temperature) and for the hydrodynamics. For the scalars, if diffusive transport is neglected at the boundary and if an upwind scheme is used at the boundary, the concentration outside the domain is needed only when the fluid is moving inside. In tidal systems, the direction of the flow is periodic, and it is possible that fluid that moved out during the last part of the ebb tide will move in during the first part of the flood. In order to account for this, the model allows the value of the boundary to be modified by using a decaying time. Hydrodynamic boundary conditions are usually imposed in terms of flow rates, or in terms of levels. The former are generally used at river boundaries, while the latter are used at the ocean boundary, where the level is easier to measure than the flow rates. In open boundaries, the level at the boundary can be modified by the solution inside the model, both when the flow moves in and when it moves out. In both cases, difficulties are similar, because the velocity of the propagation of perturbations of the level is different from the velocity of the flow. To deal with this problem, radiative boundary conditions must be used. The aim of the radiation condition is to compute the surface level at the boundary as a function of the waves that are moving inside (which must be known), and of those pro-

duced inside the domain and moving outside (which the model must be able to identify). An extensive analysis of the use of such a boundary condition is described in Santos and Neves (1991). Another kind of boundary condition is the sponge layer. The use of sponge layers, in order to dampen out waves and other disturbances generated in the interior of the computational domain, is fairly common in atmospheric models. The main feature of this condition is the addition of extra grid elements where the bottom friction coefficient and the vertical viscosity are increased exponentially from their interior value to four times that value at the outer edge of the sponge. For bottom friction, the following formula was used:

$$R_s = R_f \{\exp[b(50\,000 - x)]\};\ 50\,000 \geq x \geq 0 \quad [11]$$

where R_s is the bottom friction coefficient within the sponge and b is a factor determined so as to give $R_s = 4R_f$ at the outer edge of the sponge. In the present paper, a sponge layer 50 km wide is added to the grid at the left boundary.

Methodology

MOHID3D was implemented in the Northeast Atlantic (30° N to 60° N and 5° E to 25° W) with a high local resolution in the slope and shelf regions. To investigate the north-south density gradient as the driving mechanism for the poleward current, the model was first forced with Levitus's (1982) climatological data. Climatological winds (Hellermann and Rosenstein, 1983) were then applied to study the role of wind-stress on the modification of the flow along the coastal and slope regions of western Europe. The spatial step of the model varies from 40 km near the boundaries to 8 km near the continental shelf and slope. The model has 14 layers in the vertical, with an interface at 200 m. The upper sigma domain has 8 equal layers, and the lower domain the remaining 6. Each of the first 5 layers of the lower domain represents 10 percent of the depth below 200 m.

RESULTS

Density-driven experiments

In the present paper, we describe results obtained for typical spring and autumn conditions. Figures 1 and 2 show the circulation at two levels, obtained by forcing the model only with climatological density fields. This numerical experiment shows that the density distribution is able to produce a poleward flow, with seasonal variations that reaches the surface both in spring and autumn. This was the expected result, if we believe that the current is reversed during the upwelling season due to the wind action. It is suggested that the slope current is continuous along the European Margin, from the Portuguese to the Irish slopes. The transport increases poleward, both along Portuguese and Celtic-Armorican slopes, and decreases along the northern Spanish slope. In the upper layers of the model, northward maximum current speed is about 10 cm s^{-1} at 39° N and 20 cm at 42° N. This agrees with the theory predicting that cross-slope sea level is proportional to along-slope distance in regions where bottom friction plays a minor role. We expected this to happen along the Portuguese/northwest Spanish coast. Bottom friction may be important in northern regions (e.g., off the Hebrides) where the flow is fully developed. On the slopes of northern Spain, poleward changes in density do not force the current, and bottom friction becomes important, causing the transport to decrease. Typically, the core of the current is found between 500-1 000 m in depth, corresponding to the shelfward divergence of isopycnals.

During the spring, the current rapidly decreases, both shelfward and offshore. This result agrees with the Huthnance (1984) theory (see equation [1]). Figure 3 shows a comparison between along-slope current obtained with equation [1] –considering a surface slope corresponding to south-north density gradient 0 (10^{-7}), a thermal layer depth of 1 000 m and a friction coefficient 0 (10^{-4})– and interpolated model currents at 39° N for corresponding water depths. A considerable degree of agreement is obtained. The current is confined to the slope regions, following the depth contours. During the autumn, the current is stronger and broader, spreading over the shelf. Its orientation along the depth contours is not clear.

Spring climatological winddriven experiments

In this experiment, after an initial adjustment to the Levitus density field, climatological spring

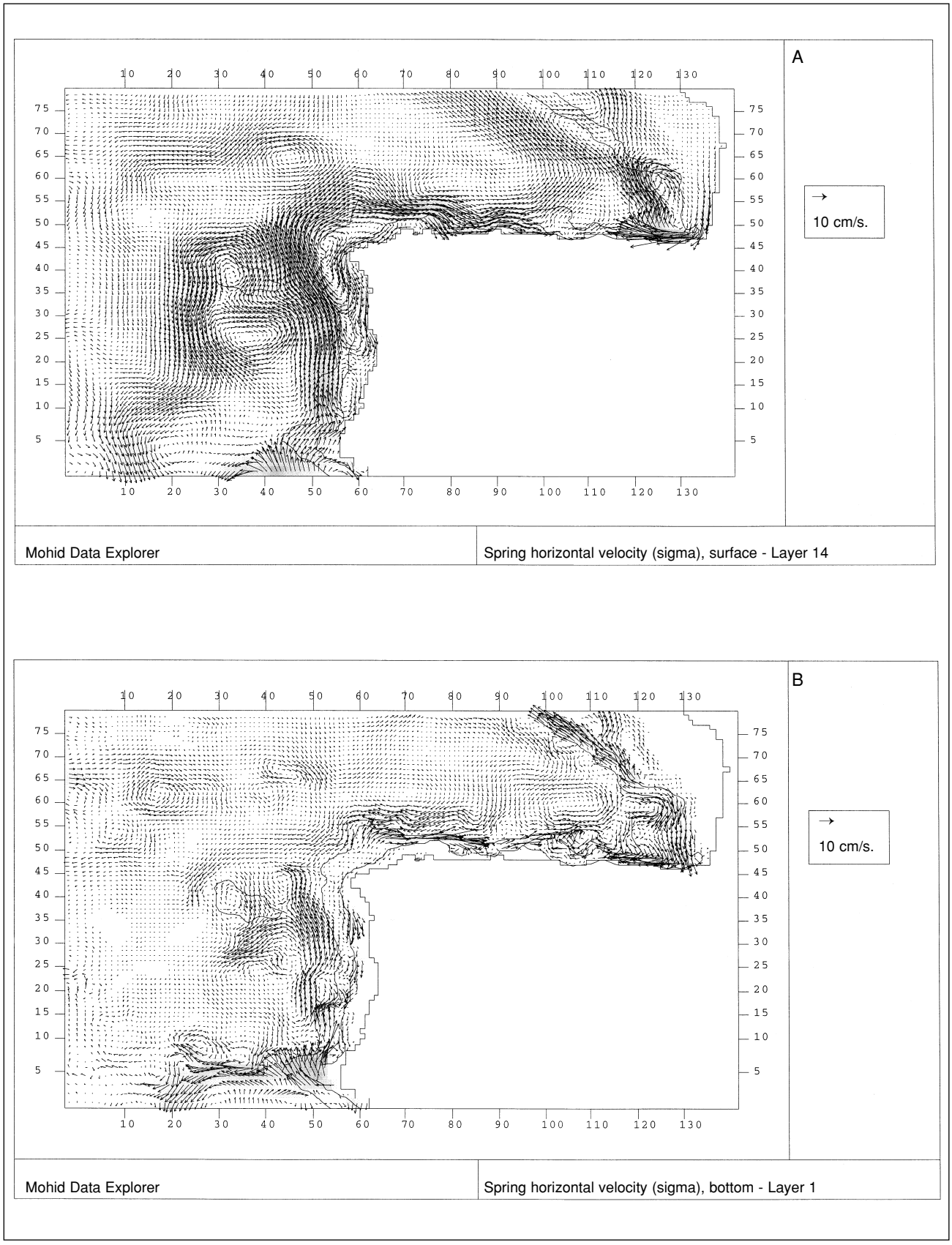

Figure 1. (A): velocity field at surface for the spring simulation; (B): velocity field at bottom sigma layer for the spring simulation

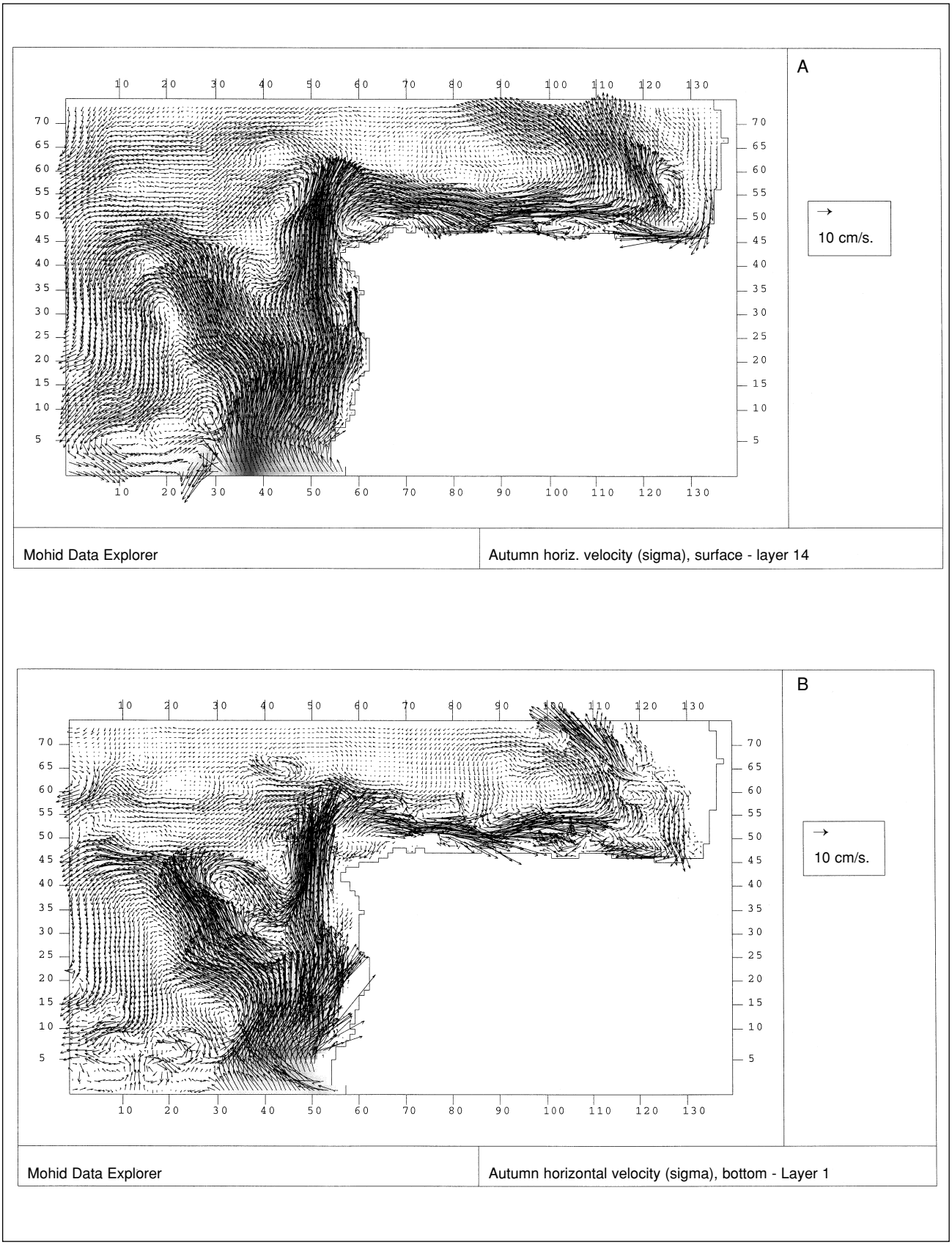

Figure 2. (A): velocity field at surface layer for the autumn simulation; (B): velocity field at bottom sigma layer for the autumn simulation

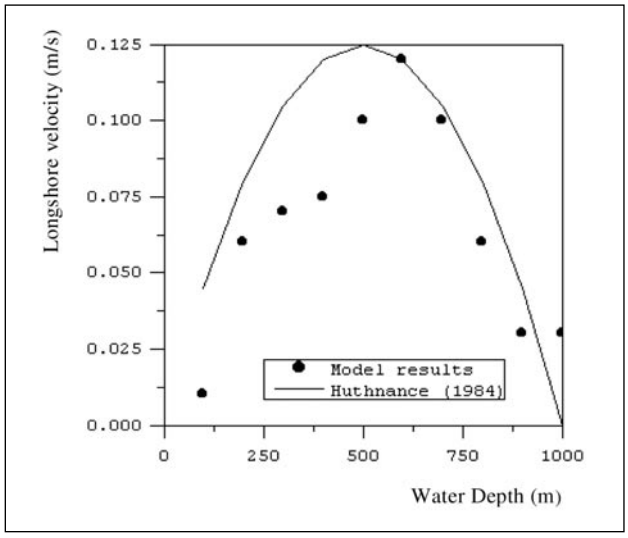

Figure 3. A comparison between theoretical and modelled along-slope current at 39° N

wind (Hellerman and Rosenstein, 1983) is imposed. In this situation, the flow is reversed in the surface layers under the influence of the southward winds. The poleward undercurrent is found below this surface layer and is concentrated on the slope, following the depth contours (figure 4). Cross sections at 42° N shows that the current extends for about 100 km off the shelf-break (figure 5). Two maximums are consistently found, both in spring and in autumn (figure 6) –one in the upper levels offshore and other at lower levels inshore. Probably the occurrence of these cores of maximum speed is due to the importance of the baroclinic component of the current. The vertical extension of the current is about 1 200 m, from 1 500 m depth (the depth of MIW) to the bottom of the surface layer.

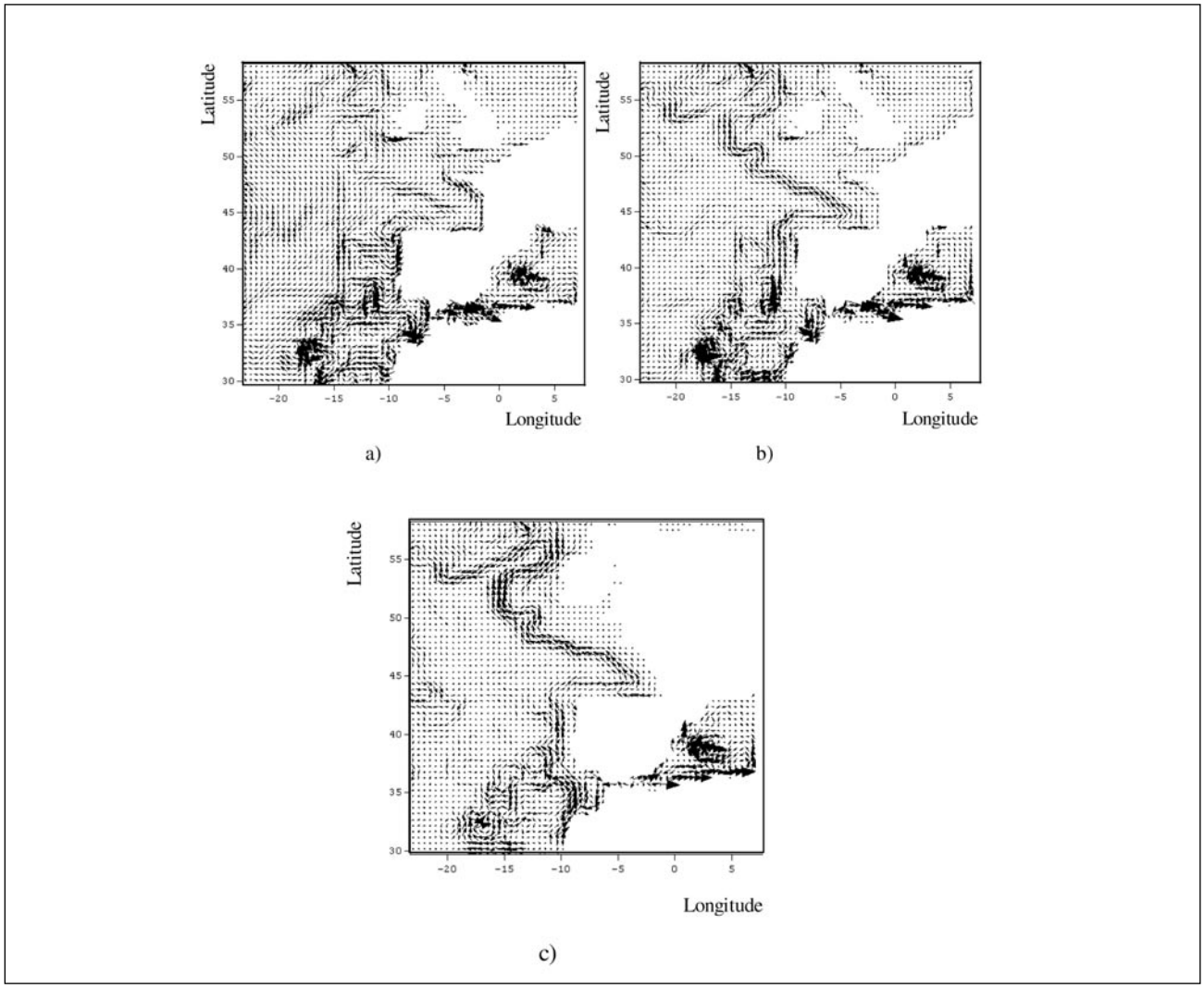

Figure 4. Spring wind-driven velocity range at: (a): surface; (b) layer 7; (c) layer 2

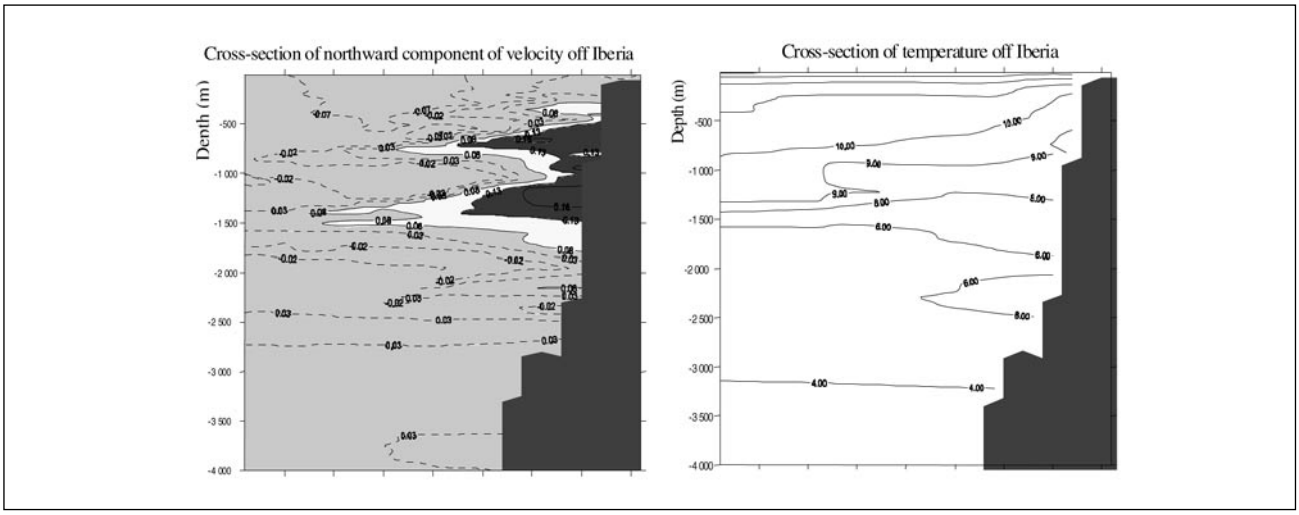

Figure 5. Cross section of northward component of velocity and density at 41° N in the spring

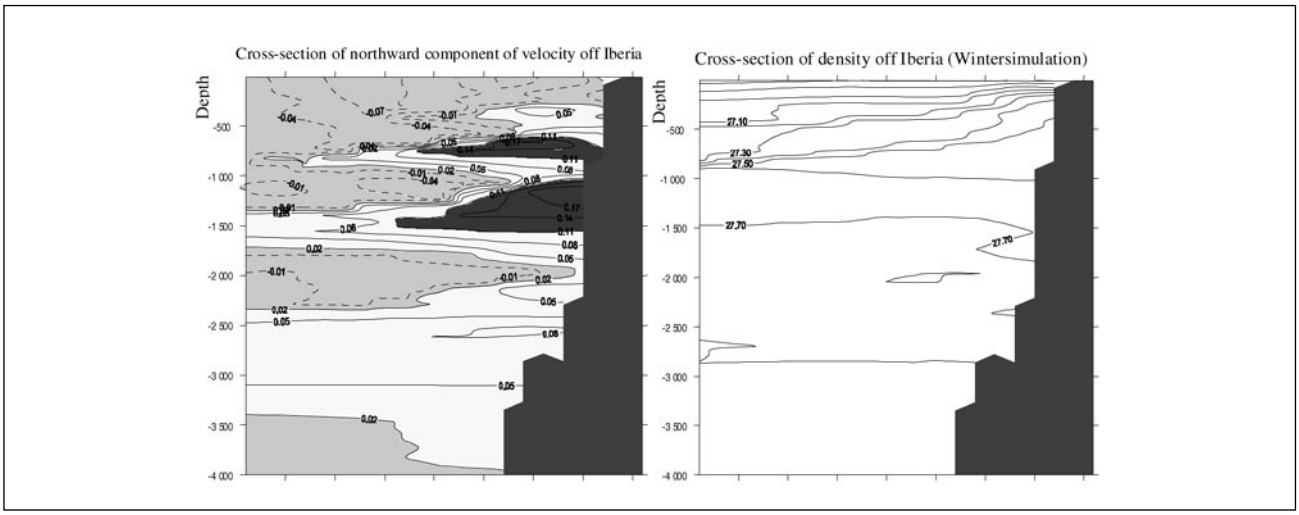

Figure 6. Cross section of northward component of velocity and density at 41° N in the autumn

DISCUSSION

Our findings indicate that thermohaline forcing can drive a poleward current along the European slopes. The currents obtained with the numerical model MOHID3D reasonably agree with the analytical model of Huthnance (1984), revealing that JEBAR (Joint Effect of Baroclinicity and Relief) is probably the main driving mechanism. However, the re-adjustment to geostrophic eastward flow is probably also important for the generation of the poleward current. Wind-stress curl (not studied in the present paper) may also be important, mainly in the spring, when it is markedly cyclonic.

It is suggested that the autumn/winter surfacing of the undercurrent may be caused by the weakening/reversing of the wind. Lynn and Simpson (1987) proposed a similar theory for the poleward current off California.

The volume transport associated with the current obtained increases poleward, and is mainly concentrated on the slope regions. Maximum speeds, lateral and vertical extensions and seasonal variability are in the range of observations.

ACKNOWLEDGEMENTS

The Commission of the European Communities, under contract MAS2-CT93-0069, supported this re-

search. The first and third authors were partially supported by grants made available by the Junta Nacional de Investigação Científica e Tecnológica (JNICT), under contract PRAXIS XXI/BM/637/94 and PRAXIS XXI/BM/1223/94, respectively.

REFERENCES

Abbott, M. B., A. Damsgaard and G. S. Rodenhuis. 1973. System 21, Jupiter: A design system for two-dimensional nearly-horizontal flows. *J. Hydraul. Res.* 1: 1-28.

Ambar, I. J. 1984. Seis meses de medições de correntes, temperaturas e salinidades na vertente continental ao largo da costa alentejana. Grupo de Oceanografia. Universidade de Lisboa. *Technical Repport* 1/84: 47 pp. Lisbon.

Ambar, I. J. 1985. Seis meses de medições de correntes, temperaturas e salinidades na vertente continental Portuguesa a 40° N. Grupo de Oceanografia. Universidade de Lisboa. *Technical Repport* 1/85: 40 pp. Lisbon.

Ambar, I., A. F. G. Fiúza, T. Boyd and R. Frouin. 1986. Observations of a warm oceanic current flowing northward along the coasts of Portugal and Spain during Nov-Dec 1983. *EOS Transaction. American Geophysical Union* 67 (144): 1 054 pp.

Backhaus, J. O. 1985. A three-dimensional model for the simulation of shelf sea dynamics. *Dtsch. Hydrogr. Z.* 38: 165-187.

Bakun, A. and C. S. Nelson. 1991. The seasonal cycle of wind-stress curl in subtropical eastern boundary current regions. *J. Phys. Oceanogr.* 21: 1815-1834.

Barton, E. D. 1989. The poleward undercurrent on the eastern boundary of the subtropical North Atlantic. In: *Poleward Flows Along Eastern Ocean Boundaries* (Coastal and Estuarine Studies). S. J. Neshyba *et al.* (eds.) 34: 82-92. Springer-Verlag, New York.

Beckers, J. M. 1991. Application of the GHER 3D general circulation model to the Western Mediterranean. *Journal of Marine Systems* 1: 315-332.

Cancino, L and R. J. J. Neves. 1994. 3D numerical modelling of cohesive suspended sediment in the western Scheldt estuary (The Netherlands). *Netherlands Journal of Aquatic Ecology* 28 (3-4): 337-345.

Clarke, A. 1989. Theorectical Understanding of Eastern Ocean Boundaries Poleward Undercurrents. In: *Poleward Flows Along Eastern Ocean Boundaries* (Coastal and Estuarine Studies). S. J. Neshyba *et al.* (eds.) 34: 26-39. Springer-Verlag, New York.

Coelho, H. S., A. dos Santos, T. Leal Rosa and R. J. J. Neves. 1994. Modelling the wind driven flow off Iberian Peninsula. *Gaia* 8: 71-74.

Coelho, H. S., A. dos Santos, T. Leal Rosa and R. J. J. Neves. 1994. Upwelling in the Iberian coast. In: *Modelling of Coastal and Estuarine Processes* (Estudos de Engenharia Civil). F. S. Santos and A. Temperville (eds.) 6: 225-234. Coimbra.

Frouin, R., A. Fiúza, I. Ambar and T. J. Boyd. 1990. Observations of a poleward surface current off the coasts of Portugal and Spain during the winter. *J. Geophys. Res.* 95: 679-691.

Haynes, R and E. D. Barton. 1990. A poleward flow along the Atlantic coast of the Iberian peninsula. *J. Geophys. Res.* 95: 11425-11141.

Hellerman, S. and M. Rosenstein. 1983. Normal monthly wind stress over the world ocean with error estimates. *J. Phys. Oceanogr.* 13: 1093-1104.

Huthnance, J. M. 1984. Slope Currents and 'JEBAR'. *J. Phys. Oceanogr.* 14: 795-810.

Huthnance, J. M. 1986. The Rockall slope current and shelf edge processes. *Proceedings of Royal Society of Edinburgh* 88: 83-101.

Klein, B. and G. Siedler. 1989. On the origin of Azores Current. *J. Geophys. Res.* 94: 6159-6188.

Leendertsee, J. J. and S. K. Liu. 1978. A three-dimensional turbulent energy model for non-homogeneous estuaries and coastal sea systems. In: *Hydrodynamics of Estuaries and Fjords*. J. C. J. Nihoul (ed.): 387-405. Elsevier. Amsterdam.

Leonard, B. P. 1977. A stable and accurate convective modelling procedure based on quadratic upstream interpolation. *Computer Methods in Applied Mechanics and Engineering* 19: 59-98.

Levitus, B. 1982. *Climatological Atlas for the World Ocean.* US Government Printing Office. *NOAA Prog. Papers* 13: 173 pp. Washington, D.C.

Lynn, R. J. and J. J. Simpson. 1987. The California current system: The seasonal variability of its physical characteristics. *J. Geophys. Res.* 92: 12947-12966.

McCreary, J. P., S. R. Shetye and P. Kundu. 1986. Thermohaline forcing of eastern boundary currents: With application to the circulation off west coast of Australia. *J. Mar. Res.* 44: 71-92.

McCreary, J. P., P. Kundu and S. Y. Chao. 1987. On the dynamics of the California current system. *J. Mar. Res.* 45: 1-32.

Neves, R. J. J. 1985. *Étude expérimentale et modélisation mathématique des circulations transitoire et résiduelle dans l'estuaire du Sado.* Doctoral thesis. Université de Liège. Liège: 224 pp.

Nihoul, J. C. J. 1982. Oceanography of semi-enclosed seas. In: *Hydrodynamics of Semi-Enclosed Seas.* J. C. J. Nihoul (ed.): 1-12. Elsevier. Amsterdam.

Pingree, R. and B. Le Cann. 1989. Celtic and Armorican slope and shelf residual currents. *Prog. Oceanogr.* 23: 303-338.

Pingree, R. and B. Le Cann. 1990. Structure, strength and seasonality of the slope currents in the Bay of Biscay region. *J. Mar. Biol.* 70: 857-885.

Rodi, W. 1980. Turbulence models for environmental problems. In: *Prediction Methods for Turbulent Flows.* W. Kollman (ed.): 299-349. Hemisphere. Washington, D.C.

Santos, A. J. P. 1995. *Modelo hidrodinâmico de circulação oceânica e estuarina.* Doctoral thesis. IST. Lisbon: 273 pp.

Santos, A. J. P. and R. J. J. Neves. 1991. Radiative artificial boundaries in ocean barotropic models. In: *Computer Modelling in Ocean Engineering 91.* J. Arcilla *et al.* (eds.): 373-383. Balkerna. Rotterdam.

Thompson, R. O. R. Y. 1984. Observations of the Leeuwin Current off Western Australia. *J. Phys. Oceanogr.* 14: 623-628.

Thomson, R. E. and W. J. Emery. 1986. The Haida Current. *J. Geophys. Res.* 91: 845-861.

Weaver, A. J. and J. H. Middleton. 1990. An analytic model for the Leeuwin Current off western Australia. *Continental Shelf Research* 10: 105-122.